Fiber-optic infrared reflectance spectroelectrochemistry: isomerization of a manganese pyranyl complex

Michael J. Shaw [a,*], Robert L. Henson [a], Steven E. Houk [a], Justin W. Westhoff [a], Myron W. Jones [b], George B. Richter-Addo [b]

[a] *Department of Chemistry, Box 1652, Southern Illinois University Edwardsville, Edwardsville, IL 62026, USA*
[b] *Department of Chemistry and Biochemistry, University of Oklahoma, 620 Parrington Oval, Rm 208, Norman, OK 73019, USA*

Received 16 April 2002; received in revised form 16 July 2002; accepted 8 August 2002

Abstract

A simple apparatus for fiber-optic reflectance FTIR spectroelectrochemical measurements is described. The method is useful for observing the products of electrode reactions generated in steady-state at an electrode surface, and the problem of large thin-layer resistance in non-aqueous solvents is minimized. Cyclic voltammetry (CV) and FTIR spectroelectrochemical measurements on five compounds ($[(\eta^5\text{-}C_5H_5)Fe(CO)_2]_2$ (Fp_2), $Fp(C{\equiv}CPh)$, $Mn_2(CO)_{10}$, $BrMn(CO)_5$ and (η^5-2,4-diphenyl-6-methylpyranyl)tricarbonylmanganese ($PyrMn(CO)_3$) are presented. As expected, $Mn_2(CO)_{10}$ and $BrMn(CO)_5$ are both reduced to the known $Mn(CO)_5^-$ anion, but Fp_2 is reduced in CH_2Cl_2 to form $FpCH_2Cl$, and $Fp(C{\equiv}CPh)$ forms a $[\mu^2\text{-}\eta^1\text{:}\eta^2\text{-}Fp_2C{\equiv}CPh]^+$ cation. Upon oxidation of the $PyrMn(CO)_3$ complex, the $Mn(CO)_3^+$ unit undergoes migration from the pyranyl ring to a phenyl ring to form an η^6-arene complex which has a pyrylium ion as a substituent on the arene ligand.

Keywords: Fiber-optic; FTIR spectroscopy; Spectroelectrochemistry; Organometallic; Isomerization

1. Introduction

The combination of spectroscopy and electrochemistry is a powerful tool in the investigation of redox-mediated structural changes [1,2]. Many types of spectroscopy have been coupled with electrochemistry [3,4] and in particular, IR spectroscopy has received its fair share of attention [5]. A popular method for IR spectroelectrochemistry is based on optically transparent thin layer electrode (OTTLE) cells [6,7], which often use indium–tin oxide windows, or gold or platinum grids as the working electrode sandwiched between salt plates [8,9]. Studies have also been performed using attenuated total internal reflectance (ATIR) cells [10]. These methods are appropriate for studies which examine the structural changes which accompany redox processes at the surface of an electrode.

More recently, fiber-optic methods have been used to observe chemical reactions [1,11,12] and sample the products of a bulk electrolysis in-situ [13]. This method allows for easy control of temperature, and voltammetric analysis of the bulk solution on which the spectroscopic measurements were taken without complications due to high thin-layer resistance effects accompanying the use of non-aqueous solvents [13].

This paper describes the first use of the fiber optic method in reflectance mode, which permits IR spectra of species generated at the electrode surface to be obtained.

2. Experimental

Solvents were dried over CaH_2 and freshly distilled before use. All work was performed under an atmosphere of prepurified dinitrogen. $Mn_2(CO)_{10}$ was obtained from Alfa-Aesar, $[(\eta^5\text{-}C_5H_5)Fe(CO)_2]_2$ (Fp_2) was obtained from Pressure Chemicals. $Fp(C{\equiv}CPh)$ [14], FpI [15], $BrMn(CO)_5$ [16] and (η^5-2,4-diphenyl-6-methylpyranyl)tricarbonylmanganese [17,18] were pre-

* Corresponding author. Fax: +1-618-850-3556
E-mail address: michsha@siue.edu (M.J. Shaw).

pared by literature methods. NBu_4PF_6 was obtained from Aldrich and was used as received.

Electrochemical measurements were recorded using a CV50W potentiostat available from Bioanalytical Systems of West Lafayette, IN, USA. Spectroscopic measurements were performed using a Bruker Vector 22 FTIR spectrometer equipped with a mid-IR fiber-optic dip probe and liquid nitrogen cooled MCT detector, all available from RemSpec Corporation of Sturbridge, MA, USA. The spectrometer was set to 4 cm^{-1} resolution. Typically 16 scans from 2500 to 1500 cm^{-1} were recorded but for weak signals a smaller frequency window was used with a larger number of scans. The outer PTFE (polytetrafluoroethylene) sheath on a BAS 1.6 mm diameter Pt disk electrode was shaved down on a lathe to an outer diameter of 5.0 mm for a length of 1.5 cm from the end of the electrode to allow it to fit into the end of the fiber-optic probe in place of the usual stainless steel mirror present in the transmission cell configuration. A cell similar to those used for UV–vis fiber-optic reflectance measurements was used [1]. For all experiments, a silver wire coated with silver chloride was used as the reference electrode and a platinum wire served as the auxiliary electrode. All experiments were performed in 0.15 M NBu_4PF_6 in CH_2Cl_2 at 20 °C, conditions where 1.0 mM Cp_2Fe displayed a redox couple at 0.37 V.

In a typical experiment, solid supporting electrolyte (0.5 g) was placed in the bottom half of the cell after the working electrode had been loosely inserted through the O-ring seal. The top half of the cell was already attached to the fiber-optic probe by another O-ring connection. The two halves of the cell were united and the working electrode inserted into the open end of the probe until it was about 0.5 mm away from the ZnSe crystal waveguide whereupon the detector signal was about 0.40–0.45 V. The other two electrodes and a PTFE degassing tube were inserted through the small holes left in the top of the cell, and the apparatus was flushed with dinitrogen. Dichloromethane (10.0 ml) was introduced into the cell by syringe and the solution was degassed and mixed thoroughly by bubbling dinitrogen through it. At this point the detector signal was 0.21–0.24 V.

A cyclic voltammogram (CV) was recorded of the solvent and supporting electrolyte. Background IR spectra of the solution were then recorded. Enough analyte was then introduced to make a 1–3 mM solution, which was mixed thoroughly by bubbling N_2. An IR spectrum and a CV of the solution were recorded separately. Before each set of spectroelectrochemical measurements an IR background and sample were recorded to obtain a baseline for the experiment. The potentiostat was set to hold the working electrode potential at a predetermined value for 3–10 min during which spectra were recorded. *Immediately* following the electrolysis a CV was automatically recorded.

2.1. Preparation of $[Fp_2C{\equiv}CPh]BF_4$

FpI (0.30, 1.0 mmol) was stirred with $AgBF_4$ (0.19 g, 1.0 mmol) in CH_2Cl_2 (20 ml) The solution was filtered through a 1.5 cm medium porosity sintered glass frit which supported a 1.5 cm plug of Celite as an aid to filtration. To the solution was added FpC≡CPh (0.28 g, 1.0 mmol). The mixture was stirred overnight, filtered, and the filtrate was concentrated under reduced pressure to a volume of 5 ml. Diethyl ether (2 ml) was added and the mixture cooled to −30 °C overnight to yield dark red crystals (0.11 g, 24% yield) of the product.

Anal Calc. for $C_{22}H_{15}Fe_2O_4$: C, 58.07; H, 3.32. Found: C, 57.98; H, 3.30%. FT-IR (ν, Nujol, cm^{-1}) 2059, 2042, 2010 (s, ν(CO)), 1820 (ν(C≡C). ^{1}H-NMR (δ, $CDCl_3$, 300 MHz): 7.3–7.6 m (5H, Ph), 5.40 (s, 5H, C_5H_5), 5.13 (s, 5H, C_5H_5). ^{13}C-NMR (δ, $CDCl_3$, 75 MHz): 88.32 (C_5H_5), 88.13 (Fe–C_5H_5).

3. Results and discussion

The Remspec fiber-optic system was previously used as a remote-sensing transmission cell for the analysis of the bulk solution in controlled potential electrolysis experiments [13]. By replacing the usual stainless steel mirror with a platinum disk electrode (Fig. 1), the system can be used in reflectance mode to detect the changes which occur due to redox events at or near an electrode surface. While UV–vis fiber-optic reflectance spectroelectrochemical measurements have been performed, no reports of similar systems for IR spectroscopy have appeared. The system is able to detect small changes in absorbance, i.e. 0.02 absorbance units or

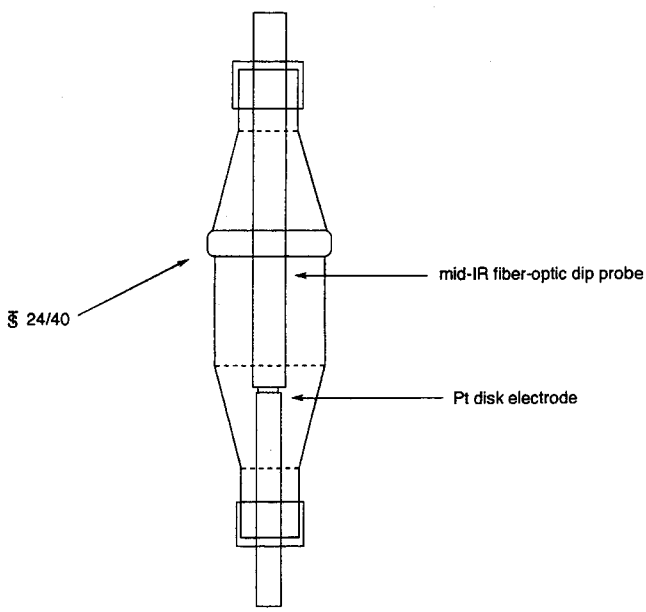

Fig. 1. Sketch of the cell system used for FTIR fiber-optic reflectance spectroelectrochemistry.

greater, with a relatively low amount of noise and it yields results which clearly show the consumption of starting material with the concomitant production of new species.

An advantage of this system over OTTLE cells and ATIR cells is the small amount of *IR* drop due to thin layer resistance. In these latter cells it is difficult to apply large positive or negative potentials to the electrodes because of resistance, especially for resistive non-aqueous solvents such as CH_2Cl_2. In our new system, the small size of the electrode means that the same potentials can be applied to the electrode for spectroelectrochemistry as can be applied during a CV scan. A representative CV experiment using this system on a 1.0 mM solution of ferrocene in CH_2Cl_2 in 0.1 M NBu_4PF_6 yielded a solution resistance of 4 kΩ as determined from the slope of a graph of peak potential versus current. While this amount of resistance may seem at first glance rather high the solvent/supporting electrolyte system is known to be rather resistive. The current which passes through the electrode during electrolysis is fairly small, on the order of 1 μA, so a representative value for the *IR* drop is therefore about 4 mV, an error which should not affect the results of the electrolysis.

The spectroelectrochemistry of several compounds, namely $Mn_2(CO)_{10}$, $BrMn(CO)_5$, $[(\eta^5\text{-}C_5H_5Fe(CO)_2]_2$ (Fp_2) and $(\eta^5\text{-}C_5H_5)Fe(CO)_2(C{\equiv}CPh)$, will be discussed to illustrate the use of the fiber-optic system. We then used this system for the characterization of a short-lived intermediate during the oxidative isomerization of (η^5-2,4-diphenyl-6-methylpyranyl)tricarbonylmanganese ($PyrMn(CO)_3$).

3.1. $Mn_2(CO)_{10}$

A CV scan of 1.1 mM $Mn_2(CO)_{10}$ at 200 mV s^{-1} revealed the expected irreversible cathodic peak at −1.87 V with an anodic daughter peak at −0.27 V [19]. This solution displayed intense IR bands at 2044, 2014 and 1978 cm^{-1}. A small amount of apparent splitting in the central band upon closer examination was found to be due to a feature in the baseline and verified by comparison of the spectrum to that of a hexane solution of $Mn_2(CO)_{10}$. As the electrode was held at −2.0 V these bands were decreased in intensity in the difference spectrum (Fig. 2) with the concomitant growth of peaks at 1898 and 1860 cm^{-1}, indicative of the production of the $[Mn(CO)_5]^-$ species [20]. These results are consistent with the previously established chemistry for this species as described in Eqs. (1) and (2).

$$Mn_2(CO)_{10} + 2e^- \rightarrow 2Mn(CO)_5^- \quad E_{pc} = -1.87\ V \quad (1)$$

$$2Mn(CO)_5^- \rightarrow Mn_2(CO)_{10} + 2e^- \quad E_{pa} = -0.27\ V \quad (2)$$

The CV recorded immediately after the electrode was held at the starting potential for 3 min revealed no new features, thereby indicating good chemical reversibility.

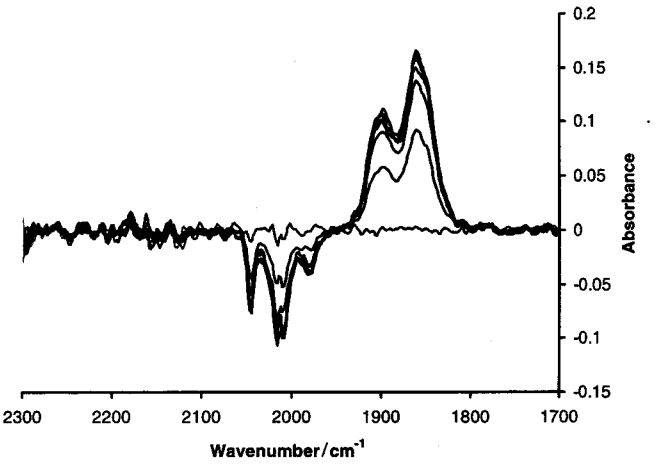

Fig. 2. Difference IR spectra of the reduction of $Mn_2(CO)_{10}$ in CH_2Cl_2.

3.2. $BrMn(CO)_5$

A 200 mV s^{-1} CV scan of 1.1 mM $BrMn(CO)_5$ revealed the expected [19] irreversible cathodic peak at −1.50 V versus Ag | AgCl and an anodic daughter peak at −0.27 V versus Ag | AgCl. This solution displayed intense IR bands at 2054 and 2046 cm^{-1}. The electrode potential was set to −1.7 V versus Ag | AgCl and the starting material bands decreased in intensity and peaks at 1900 and 1857 cm^{-1} grew in (Fig. 3). These peaks are again indicative of the production of the $[Mn(CO)_5]^-$ species as described in Eqs. (3) and (4).

$$BrMn(CO)_5 + 2e^- \rightarrow Mn(CO)_5^- + Br^- \quad E_{pc} = -1.50\ V \quad (3)$$

$$2Mn(CO)_5^- \rightarrow Mn_2(CO)_{10} + 2e^- \quad E_{pa} = -0.27\ V \quad (4)$$

The two peaks observed for $[Mn(CO)_5]^-$ are consistent with the D_{3h} geometry [20] and the electron-richness expected for this complex. For comparison, $Fe(CO)_5$ shows a similar pattern under the same conditions with bands at 2020 and 1999 cm^{-1}.

3.3. $[CpFe(CO)_2]_2$ (Fp_2)

Fp_2 is known to undergo an irreversible reduction at room temperature near the solvent limit in CH_2Cl_2, with the exact peak potential dependent on electrode history [21]. Setting the electrode potential of a 2.3 mM solution of Fp_2 to −2.0 V results in consumption of the bands due to the *cis* and *trans* terminal CO ligands (1994 and 1949 cm^{-1}) and bridging CO ligands (1774, 1768 cm^{-1}) of the Fp_2-dimer. The bands which grow in at 2021 and 1965 cm^{-1} reach their final steady-state height within 20 s of the application of the potential (Fig. 4). These new bands are at higher frequencies than the terminal IR

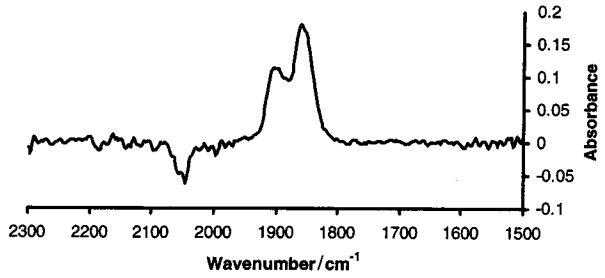

Fig. 3. Difference IR spectra after reduction of $BrMn(CO)_5$ in CH_2Cl_2 at −1.6 V vs. Ag | AgCl.

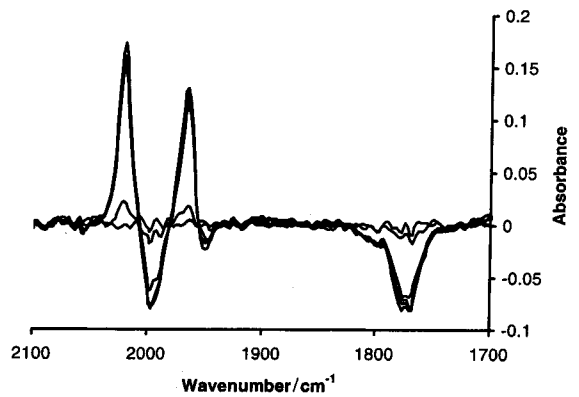

Fig. 4. Difference IR spectra of a CH_2Cl_2 solution of Fp_2.

bands of the Fp_2 dimer rather than in the 1800–1900 cm^{-1} range expected for the Fp^- anion, and they probably result from the reaction of electrode-generated Fp^- with the solvent to produce the known Fp–chloromethyl complex (ν(CO) = 2026, 1967 cm^{-1}) [22] as shown in Eqs. (5) and (6).

$$Fp_2 + 2e^- \rightarrow 2Fp^- \quad (5)$$

$$Fp^- + CH_2Cl_2 \rightarrow Fp(CH_2Cl) + Cl^- \quad (6)$$

While the $Mn(CO)_5^-$ anion appears stable in CH_2Cl_2 for the 3 min over which spectra are recorded, Fp^- quickly reacts with CH_2Cl_2 to yield the $Fp(CH_2Cl)$ complex. Given the utility of both the Fp^- and $Mn(CO)_5^-$ anions in the preparation of the corresponding metal alkyl complexes from alkyl halides, the difference in reactivity is at first glance unexpected, but can be rationalized by considering the fact that $Mn(CO)_5^-$ is a less potent reducing agent than Fp^- [21].

An anodic feature at 0.66 V along with other small peaks due to daughter products of oxidation was also observed in the CVs of the Fp_2 solution. Oxidation of the Fp-dimer at 0.66 V versus Ag | AgCl resulted in no change in the IR spectra, probably due to passivation of the electrode as has been observed previously [21].

3.4. Fp(C≡CPh)

This complex is air-stable indefinitely and was chosen because oxidation of Fp–hydrocarbyl species is known to cleave the Fe–C bond to form the Fp^+ cation. The CVs of a 2.8 mM solution of this complex displayed irreversible features at 1.10 and −1.12 V. Two spectroelectrochemical experiments were performed but no changes were observed in the spectra when the working electrode was set to a potential sufficient (−1.2 V) to reduce the complex. When the working electrode potential was set to 1.1 V, the starting material bands at 2040, 1992 and 2108 (C≡C) cm^{-1} were consumed. These bands were replaced by bands at 2077, 2056 and 2009 cm^{-1} (Fig. 5). These bands are indicative of the formation of a cationic Fp^+ complex, and they compare favorably to bands due to the σ, π-complex $[Fp_2(\mu^2\text{-}\eta^1{:}\eta^2\text{-}C{\equiv}CPh)]^+$ (ν(CO) 2059, 2042, 2010 cm^{-1} and ν(C≡C) 1820 cm^{-1}) complex which was subsequently prepared independently by reaction of Fp(C≡CPh) with $FpBF_4$. The corresponding pentamethylcyclopentadienyl complex is known to have CO bands at 2020, 1990, and 1976 and is fluxional in contrast to the Cp-derivative prepared for these studies [14]. Thus, in this case the oxidation of the alkynyl complex results in partial loss of the alkynyl group followed by coordination of the cationic iron fragment to the triple bond of the starting material.

3.5. (2,4-Diphenyl-6-methylpyranyl)tricarbonylmanganese (PyrMn(CO)$_3$)

With the utility of the fiber-optic method of examining species generated at the electrode surface established, the method was used to explore a reaction which has a product which persists only for less than a minute. The $PyrMn(CO)_3$ complex, undergoes a two-electron irreversible oxidation at E_{pa} = 0.82 V (Fig. 6). This oxidation remains irreversible even at −40 °C at 200 V s^{-1}, in contrast to the reversible behavior observable for $CpMn(CO)_2L$ complexes (L = CO, phosphines) [23]. Controlled potential electrolysis experiments confirm

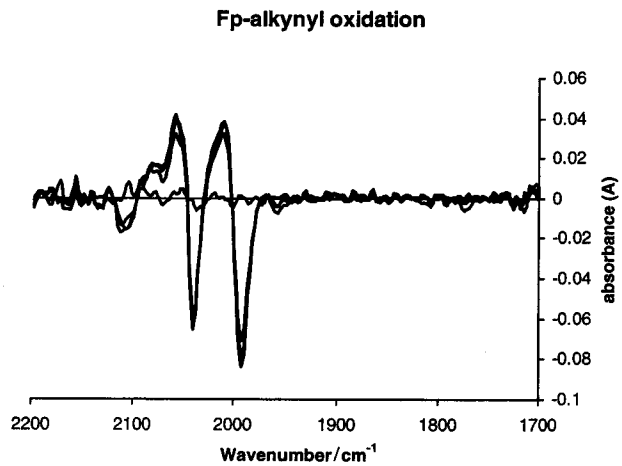

Fig. 5. Difference IR spectra of the oxidation of Fp(C≡CPh) in CH_2Cl_2.

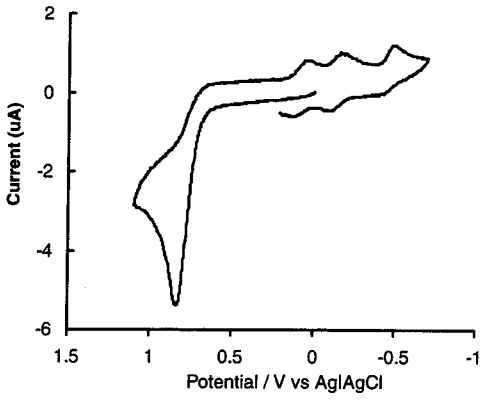

Fig. 6. CV of 1.0 mM $PyrMn(CO)_3$ in CH_2Cl_2 at 200 mV s^{-1}.

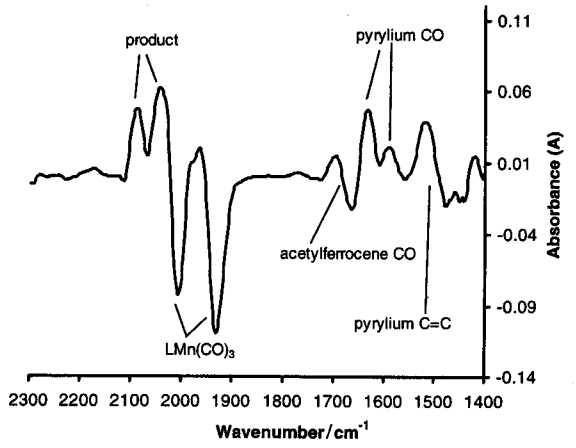

Fig. 7. Difference IR spectra of the oxidation of $PyrMn(CO)_3$ in CH_2Cl_2.

the two electron nature of the oxidation of $PyrMn(CO)_3$, but the only products obtained were the free 2,4-diphenyl-6-methylpyrylium salt, $Mn_2(CO)_{10}$ and insoluble matter which contained presumably inorganic manganese salts. NMR tube reactions which used $AgPF_6$ as an oxidant at low temperatures yielded similar results.

Cyclic voltammetric studies of the oxidation of the $PyrMn(CO)_3$ complex reveal two daughter products (Fig. 4). The two chemically reversible features at 0.06 and −0.15 V are assigned to one product and the irreversible reduction at more negative potentials is assigned to the other product. The cathodic current ratio of these daughter peaks remains constant over the scan rates of 0.05–10 V s^{-1}, which indicates that these products are formed rapidly after the oxidation, and that one product does not turn into the other on the CV timescale. One product is the free pyrylium ion which can be detected as an irreversible reduction at $E_{pc} = -0.51$ V [24]. The reduction potential matches that of authentic samples of 2,4-diphenyl-6-methylpyrylium tetrafluoroborate prepared by literature methods [25], and is close to the reduction potential of the 2,4,6-triphenylpyrylium tetrafluoroborate salt ($E^\circ = -0.39$ V) recorded under the same conditions. The other daughter product displays two reversible one-electron features and it does not persist under synthetic or controlled potential electrolysis conditions, even at low temperature so in-situ spectroelectrochemical analysis at the electrode surface was necessary to gain more information about its structure.

Oxidation of a solution of $PyrMn(CO)_3$ at 1.25 V results in the loss of its bands at 1930 and 2005 cm^{-1} and the growth of bands at 2042 and 2090 cm^{-1} as shown in Fig. 7. In addition, weaker bands at 1630, 1585 and 1514 cm^{-1} are observed to grow, which are consistent with the presence of pyrylium salts. A small peak at 1960 cm^{-1} may indicate the presence of another, shorter-lived metal carbonyl species. These studies were performed in the presence of a small amount of acetylferrocene which served as an internal standard for both the CV and IR studies. As expected, the internal standard was oxidized and its IR band shifted from 1665 to 1700 cm^{-1}.

No $Mn_2(CO)_{10}$ was detected under these conditions. The only products appear to be pyrylium salts and a cationic $(arene)Mn(CO)_3^+$-type complex which presumably still displays local C_{3v} symmetry as shown in Eq. (7). The positions of the product IR bands are consistent with those of related arenemanganese tricarbonyl complexes [26].

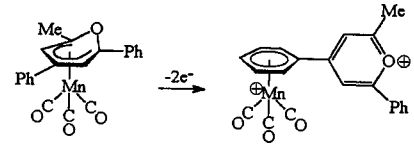

(7)

Since the cationic pyrylium ion is a poor π-ligand owing to its positive charge, it is likely that the $Mn(CO)_3$ unit migrates to a phenyl ring as shown in Eq. (7), or it falls off the ligand completely. Note that the product complex is dicationic overall, but can be viewed as an $(arene)Mn(CO)_3^+$ complex which has a cationic pyrylium substituent on the arene ring. Importantly, the monocationic chromium analogue has been prepared by another route and has been characterized crystallographically [27]. The fact that the dicationic manganese complex does not persist under synthetic conditions is consistent with the fragile nature of the arene–$Mn(CO)_3$ bond with electron-poor arenes. Electron-poor arenes do not coordinate well to the $Mn(CO)_3^+$ unit [28], and in fact, only recently have examples of $(arene)Mn(CO)_3^+$ complexes been isolated where there is a resonance-electron withdrawing group present on the ring [29].

Preliminary DFT calculations favor the 4-phenyl group as the site for migration owing to repulsion between the O-atom and the Mn-atom after two-electron oxidation of the starting material [30]. The

[11] M.L. Myrick, J. Kolis, E. Parsons, K. Chike, M. Lovelace, W. Scrivens, R. Holliday, M. Williams, J. Raman Spectrosc. 25 (1994) 59.
[12] W.R. Moser, J.R. Berard, P.J. Melling, R.J. Burger, Appl. Spectrosc. 46 (1992) 1105.
[13] W.E. Geiger, M.J. Shaw, Organometallics 15 (1996) 13.
[14] A. Munetaka, T. Masako, O. Shuji, M. Yoshihiko, Organometallics 9 (1990) 816.
[15] R.B. King, Organometallic Synthesis, Vol. 1, Academic Press, New York, 1965, p. 175.
[16] M.H. Quick, R.J. Angelici, Inorg. Synth. 19 (1979) 160.
[17] B.L. Booth, R.G. Hargreaves, J. Chem. Soc. Sect. A (1970) 308.
[18] W. Tully, L. Main, B.K. Nicholson, J. Organomet. Chem. 507 (1996) 103.
[19] M.D. Morris, Adv. Electroanal. Chem. 7 (1974) 80 (and references contained therein).
[20] J.P. Bullock, M.C. Palazzotto, K.R. Mann, Inorg. Chem. 29 (1990) 4413.
[21] P. Legzdins, B. Wassink, Organometallics 3 (1984) 1811.
[22] M.L.H. Green, M. Ishaq, R.N. Whitely, J. Chem. Soc. Sect. A (1967) 1508.
[23] (a) C.G. Atwood, W.E. Geiger, T.E. Bitterwolf, J. Electroanal. Chem. 397 (1995) 279;
(b) C.G. Atwood, W.E. Geiger, J. Am.Chem. Soc. 116 (1994) 10849 (and references contained therein).
[24] (a) D. Farcasiu, A.T. Balaban, U.L. Bologa, Heterocycles 37 (1994) 1165;
(b) M.R. Detty, J.M. McKelvey, H.R. Luss, Organometallics 7 (1988) 1131.
[25] A.T. Balaban, A. Dinculescu, G.N. Dorofeenko, G. Fischer, A.V. Koblik, V.V. Mezheritskii, W. Schroth, Pyrylium Salts: Syntheses Reactions and Physical Properties, in: Adv. Heterocycl. Chem. Supplement 2, Academic Press, New York, 1982.
[26] K.L. Malisza, S. Top, J. Vaissermann, B. Caro, M.-C. Sénéchal-Tocquer, D. Senéchal, J.-Y. Saillard, S. Triki, S. Kahll, J.F. Britten, M.J. McGlinchey, G. Jaouen, Organometallics 14 (1995) 5273.
[27] B. Caro, M.-C. Sénéchal-Tocquer, D. Senechal, P. Marrec, J.-Y. Saillard, S. Triki, S. Kahlal, Tetrahedron Lett. 34 (1993) 7259.
[28] D. Prim, A. Auffrant, F. Rose-Munch, E. Rose, J. Vaissermann, Organometallics 20 (2001) 1901.
[29] A. Aufrant, D. Prim, F. Rose-Munch, E. Rose, J. Vaissermann, Organometallics 20 (2001) 3214.
[30] M.A. Cooper, Theoretical Study of Manganese Pyranyl Complexes, M.Sc. Thesis, Southern Illinois University, Edwardsville, 2002.
[31] S. Sijoon Lee, S.R. Lovelace, D.J. Arford, S.J. Geib, S.G. Weber, N.J. Cooper, J. Am. Chem. Soc. 118 (1996) 4190.
[32] L.K. Yeung, K.E. Kim, Y.K. Chung, P.H. Rieger, D.A. Sweigart, Organometallics 15 (1996) 3891.
[33] (a) Y. Huang, G.B. Carpenter, D.A. Sweigart, Y.K. Chung, B.Y. Lee, Organometallics 14 (1995) 1423;
(b) N.G. Connelly, M.D. Kitchen, J. Chem. Soc., Dalton Trans. (1977) 931.